Vorticity flux through the Yucatan Channel and Loop Current variability in the Gulf of Mexico

Lie-Yauw Oey
Princeton University, Princeton, New Jersey, USA

Received 25 March 2004; revised 13 July 2004; accepted 11 August 2004; published 9 October 2004.

[1] Recent observations (the CANEK Program [*Candela et al.*, 2002]) suggest that potential vorticity (PV) flux anomaly (VFA) at Yucatan Channel may serve as a useful indicator of Loop Current variability, including Loop Current extension, retraction, and eddy shedding. Intuitively, anticyclonic VFA extends the Loop Current into the Gulf of Mexico and cyclonic VFA causes retraction or even shedding. However, this intuition is inconsistent with PV conservation. The problem is reexamined here by careful analyses of the relation between VFA and Loop Current variability using (1) the results of a 15-year numerical simulation of shedding specified with simple forcing, and (2) CANEK and satellite observations. Both model and observations indicate that Loop Current eddy shedding or retraction tends to occur shortly (1∼2 months) after the influx of VFA at Yucatan has turned anticyclonic, and that these events are sometimes preceded by a more prolonged period of influx of cyclonic VFA. These findings suggest that contrary to intuition, influx of cyclonic VFA tends to extend the Loop Current into the Gulf, thus making the Loop Current more susceptible to retract or shed an eddy, and influx of anticyclonic VFA may then "trigger" retraction or eddy shedding. However, the Loop Current's behaviors are much more complex than can be prescribed by these simple rules. A much longer observational data set, coupled with more refined model experiments and sophisticated analyses, is required to further quantify the phenomenon. *INDEX TERMS:* 4520 Oceanography: Physical: Eddies and mesoscale processes; 4255 Oceanography: General: Numerical modeling; 4576 Oceanography: Physical: Western boundary currents; 4243 Oceanography: General: Marginal and semienclosed seas; *KEYWORDS:* vorticity flux, Loop Current, Yucatan Channel

Citation: Oey, L.-Y. (2004), Vorticity flux through the Yucatan Channel and Loop Current variability in the Gulf of Mexico, *J. Geophys. Res.*, *109*, C10004, doi:10.1029/2004JC002400.

1. Introduction

[2] It is now a well-established fact that the Loop Current in the Gulf of Mexico sheds eddies in a complicated manner, at irregular intervals of 3∼17 months [*Sturges and Leben*, 2000; *Oey et al.*, 2003, and references therein]. It is of interest (and potentially important) to relate shedding to flow parameters at the Yucatan Channel. *Candela et al.* [2002, 2003] (hereinafter referred to as C2002 and C2003) reported such an attempt based on a remarkable data set that they have obtained in the Yucatan Channel. The observations (the CANEK Program) consist of, amongst other things, 23-month current-meter and acoustic Doppler current profiler (ADCP) measurements across the channel. Using these data the authors computed the potential vorticity flux (PVF) through the channel,

$$\mathrm{PVF} = \iint vq\,dxdz, \tag{1}$$

where the double integral is taken over the channel cross section for water with potential temperature $T > 6.8°\mathrm{C}$ ($z \approx -750$ m) and q is Ertel's potential vorticity. (I follow C2002 and C2003 and reverse the sign of q so that cyclonic shear gives positive q_2. There was a typographical error in both papers; the minus sign was omitted (J. Candela, personal communication, 2004).)

$$q \approx -\left[f\frac{\partial \rho}{\partial z} + \frac{\partial v}{\partial x}\frac{\partial \rho}{\partial z} - \frac{\partial v}{\partial z}\frac{\partial \rho}{\partial x}\right]/\rho_o \quad = q_1 + q_2 + q_3. \tag{2}$$

Here, only the three dominant components of potential vorticity, q_1 (planetary), q_2 (horizontal shear), and q_3 (vertical shear) are shown. The coordinate axes are chosen such that x is positive from left to right (nearly eastward) across the channel, y is orthogonal to x (i.e., nearly northward, positive), and z is positive upward, $z = 0$ is the mean sea-surface. The (x, y) components of the velocity are (u, v), ρ is density, ρ_o is reference density, and f is the Coriolis parameter. Of the three terms in equation (2), the PV flux due to q_1, $\mathrm{PVF}_1 = \int\int vq_1 dxdz$, is largest, and C2002 found that it is unrelated to Loop Current extension and

0148-0227/04/2004JC002400

retraction variability. The flux due to q_3 is small and also unrelated to Loop Current variability. C2002 noted that the flux due to the horizontal shear term q_2,

$$\mathrm{PVF}_2 = -\int\int v\frac{\partial v}{\partial x}\frac{\partial \rho}{\partial z}/\rho_o dxdz, \quad (3)$$

is related to Loop Current variability. The authors defined the time integral of this flux, called "cumulative PV flux,"

$$\mathrm{CPVF}_2 = \int \mathrm{PVF}_2 dt, \quad (4)$$

and noted that two shedding and two Loop Current retraction events (during the 23-month period) occurred when CPVF_2 was near its local maxima indicative of maximum cumulative influx of cyclonic vorticity flux anomaly (VFA). The existence of a connection between CPVF_2 (PVF_2) and Loop Current variability is purely empirical, but it is intuitively attractive and will be assumed a priori. C2003 also reported the above PV flux analysis based on the results from two grid configurations of the Océan Parallélisé (OPA) z-level primitive equation model: one at 1/6° resolution (the ATL6 configuration) and the other one at finer 1/12° resolution (the PAM configuration). To force their models, they used daily surface fluxes from the European Centre for Medium-Range Weather Forecasts (ECMWF): 1979–1993 for the 1/6° resolution, and 1999–2001 for the 1/12° resolution. C2003 found that the 1/6° resolution model stopped shedding eddies beginning from the sixth year, so only the first 5 years (1979–1983) were used in their analysis. On the basis of these observational and model analyses, and also satellite-derived sea surface height (SSH) data, the authors concluded that "the shedding of anticyclonic eddies by the Loop Current is preceded by periods of positive (cyclonic) vorticity influx into the Gulf of Mexico that causes a retraction of the current and not by the influx and accumulation of negative (anticyclonic) vorticity that enhances the Loop Current growth and extension into the Gulf of Mexico."

[3] *Oey et al.* [2003] (hereinafter referred to as O2003) reached a different conclusion regarding the role of vorticity at Yucatan on Loop Current extension and retraction. The authors conducted several decadal (16∼32 years) numerical experiments to examine effects of external forcings on Loop Current variability and eddy shedding. Their model experiments yielded varying periods of eddy shedding, from 3 to 16 months. They attributed the short-period shedding as being caused by transport fluctuations through the Yucatan Channel, forced by remote wind-forcing over the Atlantic Ocean. O2003 noted that the shedding periods lengthened in experiments in which anti-cyclones were prevalent in the model Caribbean Sea. The model Loop Current would then tend to remain close to the Yucatan entrance and would be "less prone to shed eddies, and intervals between shedding are prolonged."

[4] O2003 attempted to rationalize these numerical model findings with a simple PV-conservation analysis on a geostrophic upper layer streamline [*Reid*, 1972]. The Reid's formula is modified so that the streamline may leave the channel with non-zero curvature. The following estimate of the northward intrusion distance 'b' of the Loop Current results:

$$b = \frac{\varsigma_o}{\beta} + \sqrt{\left(\frac{\varsigma_o}{\beta}\right)^2 + \frac{2V_c}{\beta}}, \quad (5)$$

where β is the planetary beta and ς_o and V_c are vorticity and speed, respectively, of the core current (i.e., the near-surface, fast-speed region) at Yucatan Channel. The formula is plotted in O2003's Figure 11. For a given V_c, the Loop Current retracts when $\delta\varsigma_o < 0$ and extends into the Gulf when $\delta\varsigma_o > 0$, where 'δ" denotes a (time) change. If on the other hand the ς_o is fixed and V_c varied, then the Loop Current retracts when $\delta V_c < 0$, and expands when $\delta V_c > 0$. The behavior of the Loop Current (i.e., whether or not it extends into the Gulf) as a function of δV_c is intuitively obvious, but as a function of $\delta\varsigma_o$ it seems counterintuitive. Since $(f + \varsigma)$ is conserved, a fluid parcel that is advected northward acquires negative vorticity, up to a y-point where the streamline loops eastward. With a surplus of vorticity at Yucatan (i.e., $\delta\varsigma_o > 0$) the parcel would need to trace a more northerly path (to rid its excess vorticity) than a parcel with vorticity deficit ($\delta\varsigma_o < 0$). Note that equation (5) says nothing about eddy shedding. Also, positive $\delta\varsigma_o$ can mean either ς_o is becoming less negative if $\varsigma_o < 0$, or more positive when $\varsigma_o > 0$, and vice versa for negative $\delta\varsigma_o$. O2003 suggests that eddy shedding would be more likely to occur (e.g., by flow instability or other mechanisms) when the Loop Current extends ($\delta\varsigma_o$ is positive), and vice versa when the Loop Current retracts. This idea that the Loop Current is more prone to shed eddies when $\delta\varsigma_o$ is positive is consistent with C2002's observational analysis that sheddings were sometimes observed near the end of a period of cumulative (i.e., time integral of) VFA, i.e., near a local maximum of the CPVF_2 time series. However, the intuitive idea that influx of cyclonic VFA causes the Loop Current to retract or to shed an eddy, and that influx of anticyclonic VFA extends the Loop Current into the Gulf, is in contrast to the above PV-conservation argument. To clarify these contrasting views, I examine in the following sections results of a numerical model experiment with simple forcing, and also the CANEK and satellite observations. The objectives are to elucidate the relative phasing between PVF_2 and CPVF_2, and also the relation between these PV fluxes and Loop Current variability and eddy shedding.

2. Analysis of a Model With Simple Forcing

[5] An MPI/parallelized version of O2003's primitive-equation, terrain-following model of the western north Atlantic Ocean (6°N–50°N and 55°W–98°W) is used. Grid sizes in the vicinity of the Yucatan Channel, including the northeastern Gulf of Mexico and northwestern Caribbean Sea, are approximately 10 km, and there are 25 sigma-levels in the vertical. The model is initialized with annual-mean temperature and salinity from the Generalized Digital Environmental Model (GDEM) climatology [*Teague et al.*, 1990], and steady transports are specified at 55°W according to *Schmitz* [1996]. All other boundary fluxes are nil. (The setup is the same as O2003's "experiment A.") Under

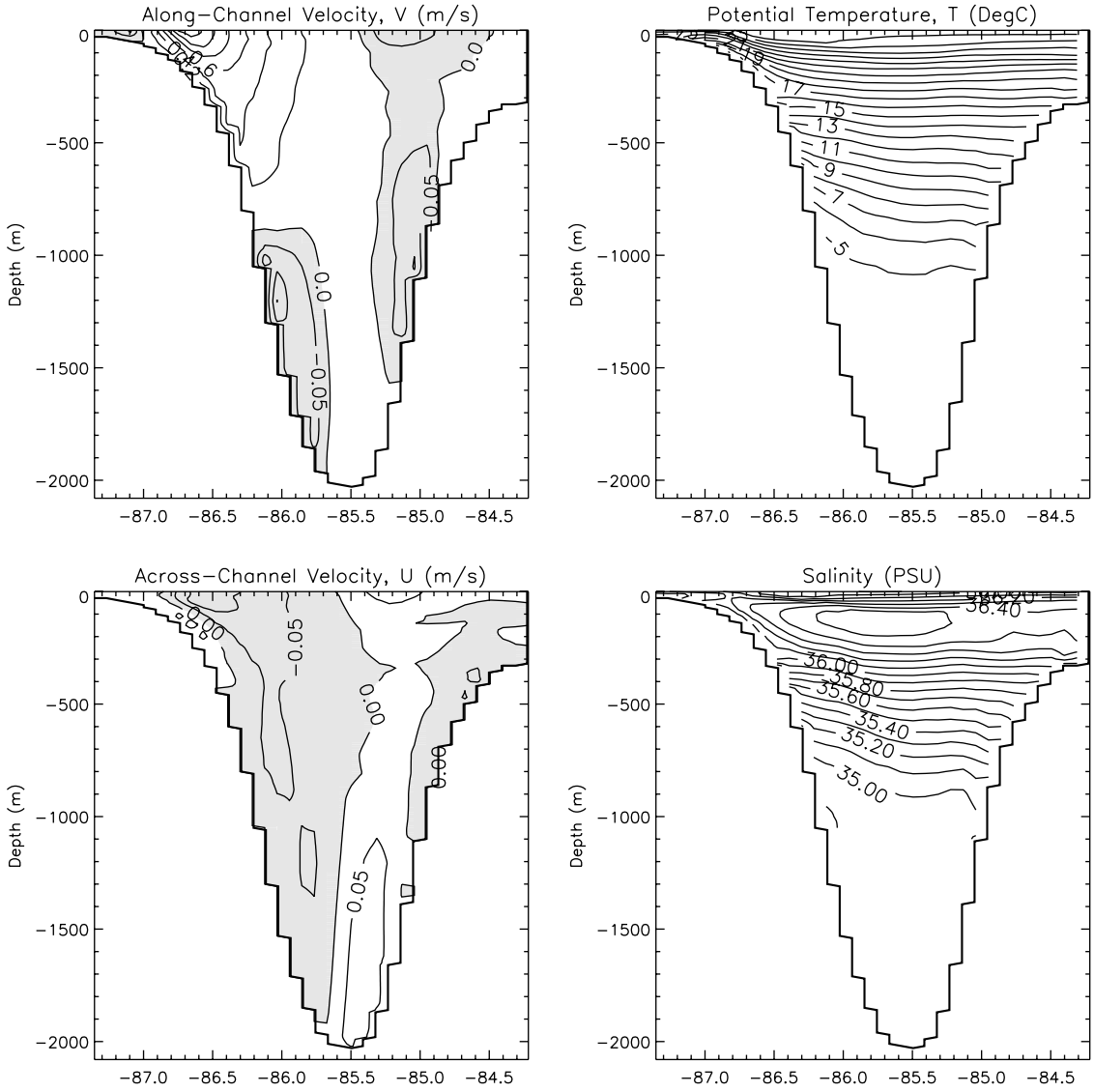

Figure 1. Vertical-section contours of 13-year mean along- and across-channel velocities, and also the potential temperature and salinity at the Yucatan Channel. Note the two scales of contour intervals for v: 0.2 m s^{-1} for $v > 0$, and 0.05 m s^{-1} for $v < 0$.

these conditions, the model produces nearly periodic eddy shedding with a period of 8∼10 months. The integration was carried out for 15 years but, to allow adjustments, the first 2 years were skipped in the analysis. Flow fields in the Yucatan Channel and times when Loop Current eddies are shed are analyzed. All variables were interpolated from the sigma-coordinate to z-coordinate, and then the PV and flux terms, etc., were calculated.

[6] The choice of a simple forcing is intentional. If the idea that fluctuations of VFA at Yucatan and Loop Current variability are related has a dynamical basis, it would likely show in a model with simple forcing. The relationship will be much more difficult to extract in models driven by more complex forcing, such as those used in C2003's OPA model and O2003's experiment C or D. One notes that the existence of VFA fluctuations (cyclonic or anticyclonic; or any unsteadiness) is not necessary for shedding, as demonstrated by *Hurlburt and Thompson* [1980]. These authors obtained shedding despite of a steady inflow specified at their model Yucatan Channel.

[7] Figure 1 shows vertical-section contours of 13-year mean along- and across-channel velocities, and also the potential temperature and salinity. The v-contours show a high-speed current core on the western part of the channel near the surface and a deep return flow. There is also return flow near the eastern portion of the channel, both near the surface and also deeper. The T-contours show characteristic frontal structure near the west, with surface outcropping just above the upper slope. Associated with the front are u-contours which show convergence over the western shelf-break. The S-contours show the characteristic Caribbean Subtropical Underwater, salinity maximum ≈ 36.57 psu at $T \approx 21.5$°C [*Elliott*, 1982] (observed maximum ≈ 36.69 psu). Despite the simple model forcing, the general structures of the v- and T-contours are similar to those shown previously [*Candela et al.*, 2002, 2003; *Oey et al.*, 2003].

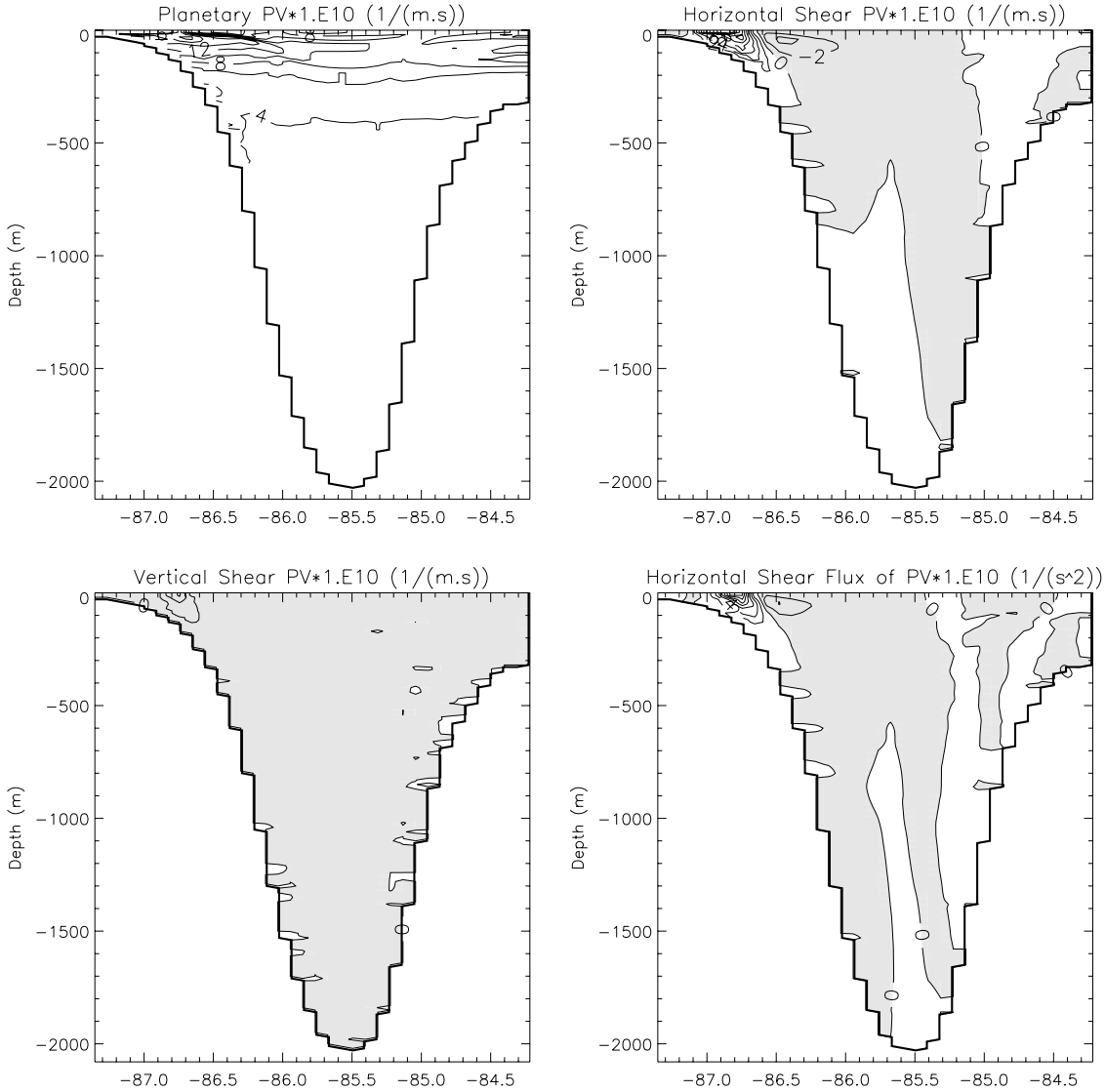

Figure 2. Vertical-section contours of 13-year mean planetary potential vorticity (PV): $-f(\partial\rho/\partial z)/\rho_o$, vertical-shear PV: $(\partial v/\partial z)(\partial\rho/\partial x)/\rho_o$, horizontal-shear PV: $-(\partial v/\partial x)(\partial\rho/\partial z)/\rho_o$, and flux of horizontal-shear PV: $-v(\partial v/\partial x)(\partial\rho/\partial z)/\rho_o$.

[8] Figure 2 shows section contours of 13-year means of the three PV terms: q_1, q_2, and q_3, as well as the vq_2 (i.e., the integrand in equation (3)). The q_1 simply reflects vertical stratification and is large near the surface. The q_2 is dominated by strong horizontal shears that exist near the surface on the western portion of the channel (see the v-contours in Figure 1). In general, positive shear to the left of the v-maximum dominates negative shear to the right. The q_3 is also largest near the surface on the western portion of the channel, but has small magnitudes in comparison to q_2. These features, in particular the dominant contribution to q_2 by shears near the surface on the western portion of the channel, are consistent with C2002's and C2003's analyses. Contours of "vq_2" reflect the q_2 values weighted by v, and show large magnitudes also near the surface on the western side of the channel. It follows that most of the contribution to PVF_2 is from those vq_2-values also near the surface on the western side, especially values in the current core. (Note that if the channel is rectangular and $\partial\rho/\partial z$ is independent of x through most of an "M-region," say, of the xz-plane, the integral in equation (3) becomes $\int_M(v_w^2 - v_e^2)d\rho/(2\rho_o) + I_S + I_B$, where subscripts "$e$" and "$w$" denote eastern and western channel walls, and I_S (I_B) is the double integral for region near the surface (bottom) where sloping isopycnals intersect the boundary. If "v" is small near the walls and the bottom, then only I_S remains.) This result suggests that the observed PVF_2 time series may also be dominated by flow values from the 2∼3 current-meter moorings and ADCP's on the western side of the channel. That the vorticity flux is dominated by flow values in the current core suggests also that C2002's (and C2003's) flux analysis and O2003's "core-streamline" PV analysis are consistent with each other (think of streamlines that emanate from the core; recall that O2003 looks at fluid parcels on streamlines that originate from the Yucatan core current, while C2002 and O2003 examine vorticity flux through the entire Yucatan section).

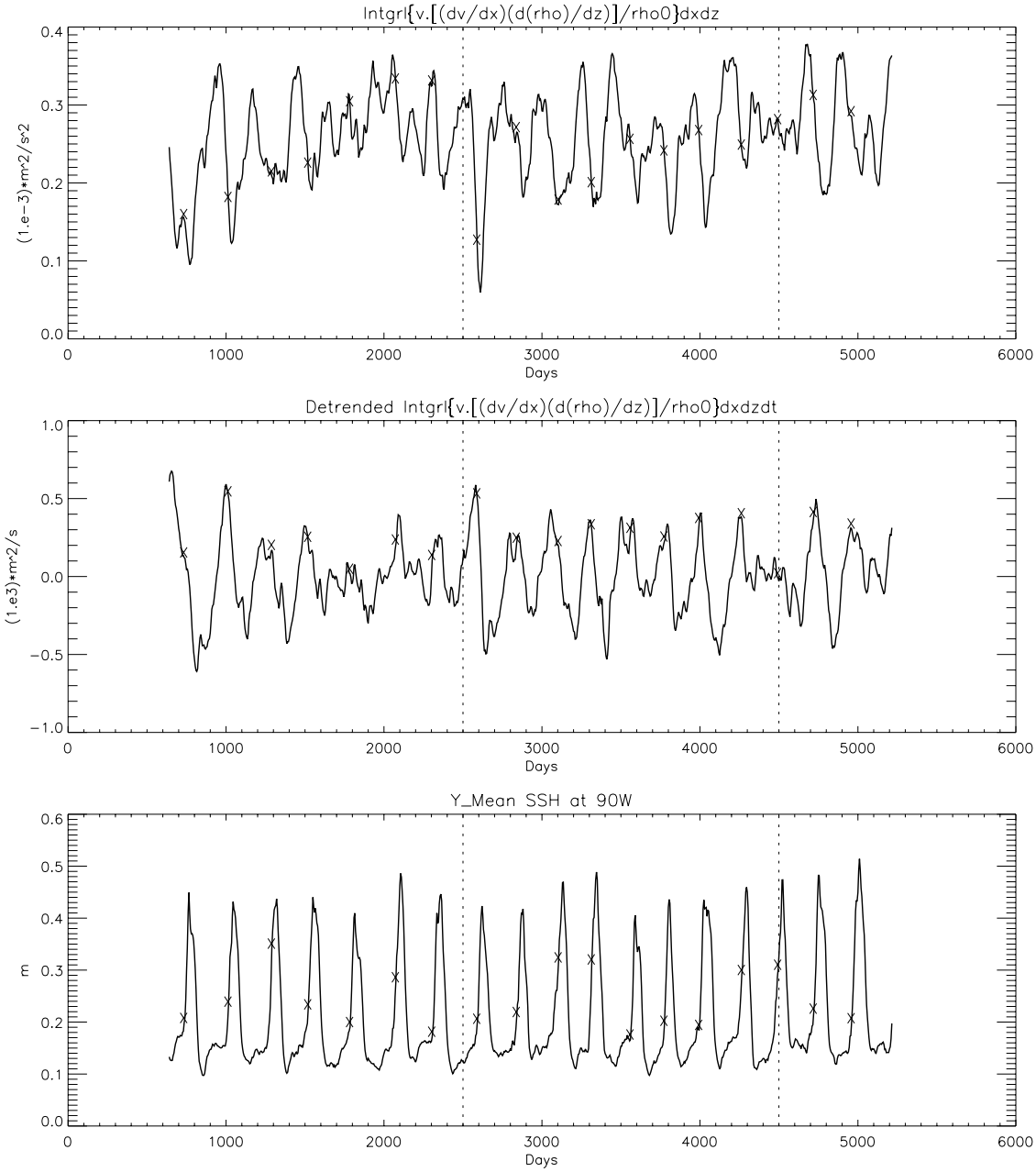

Figure 3. (top) Low-passed time series of flux of horizontal shear $PVF_2 = -\int\int v\frac{\partial v}{\partial x}\frac{\partial \rho}{\partial z}/\rho_o dxdz$, (middle) time-integral of this flux $CPVF_2 = \int PVF_2 dt$, and (bottom) the meridional-mean sea-surface height at 90°W that serves as a proxy of Loop Current eddy shedding. These time series are from a numerical simulation of Loop Current eddy shedding specified with simple forcing. The crosses on each curve indicates actual times the modeled Loop Current shed eddies. The dotted lines bracket time period for which the three curves are shown on the same plot in Figure 4a.

[9] Figure 3 gives model time series of PVF_2, $CPVF_2$ and the meridional mean of SSH at 90°W in the Gulf of Mexico. Here the PVF_2 has been low-passed to remove periods shorter than 50 days, and the $CPVF_2$ has been de-trended (following C2003). De-trending shows the highs and lows of the generally monotonic function $CPVF_2$. Note that (in the model) PVF_2 is wholly positive because of the dominant cyclonic shears on the western portion of the channel near the surface. (*Candela et al.*'s [2003] ATL6 model shows similar but mostly negative PVF_2; see their Figure 16.) Thus the anomaly, VFA, is discussed here. Assuming that stratification varies on a longer timescale than velocity and vorticity, equation (3) shows that

$$\delta(PVF_2) = -\iint [V_c\delta\zeta_o + \zeta_o\delta V_c]\frac{\partial \rho}{\partial z}/\rho_o dxdz. \qquad (6)$$

A downward "trend" in the PVF_2 curve (i.e., decreasing PVF_2, from a local maximum, say) indicates (on average over the cross section) influx of fluid parcels with

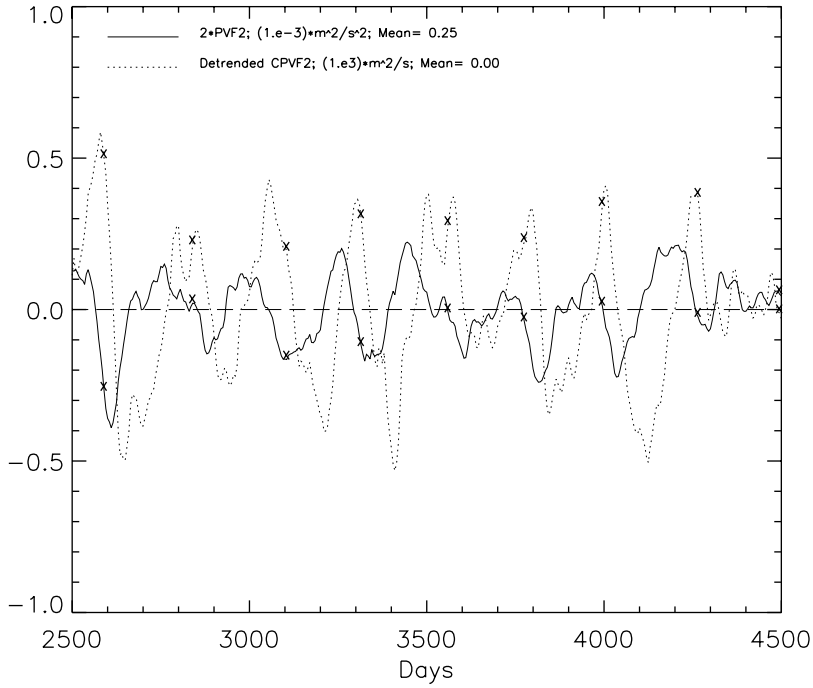

Figure 4a. Superposition of the low-passed time series of flux of horizontal shear $PVF_2 = -\int\int v\frac{\partial v}{\partial x}\frac{\partial r}{\partial z}/r_o dxdz$ (solid line) and time-integral of this flux $CPVF_2 = \int PVF_2 dt$ (dotted line) for the time period 2500–4500 days, to illustrate their relative phasing as discussed in text. The time-mean of each series is indicated and has been removed. For clarity, the PVF_2 is multiplied by 2. The crosses on each curve indicate actual times the modeled Loop Current shed eddies.

strengthening anticyclonic vorticity (or weakening cyclonic vorticity) or decreased (increased) influx of parcels with cyclonic (anticyclonic) vorticity, or both. The former relates to changes in vorticity, $\delta\varsigma_o < 0$, while the latter to changes in inflow velocity fluctuations, $\delta V_c < 0$ for $\varsigma_o > 0$ or $\delta V_c > 0$ for $\varsigma_o < 0$. The situation is reversed for an upward trend in the PVF_2 curve. For simplicity, the first situation (downward trend in the PVF_2 curve) will be referred to as influx of anticyclonic VFA, and the second situation (upward trend) as influx of cyclonic VFA. C2002 and C2003 use these same definitions for the $CPVF_2$ time series.

[10] In Figure 3, the highs in SSH time series indicate passages of Loop Current eddies past 90°W [c.f. *Hurlburt and Thompson*, 1980]. Unlike in models driven by more complex forcing (e.g., O2003's experiment C), rings in the present simulation always separate cleanly from the model Loop Current; that is, there is no eddy–Loop Current reattachment process (O2003) that can cloud the exact timing of separation. After a ring separates, it propagates west, and the SSH curve at 90°W increases to a maximum as the ring's center arrives. The times when the model Loop Current sheds eddies are determined visually from daily maps of velocity vectors and SSH. These times precede the times of SSH highs at 90°W by 26∼35 days (average ≈ 30 days) and are indicated on each curve (Figure 3) as crosses. The SSH at 90°W uniquely defines shedding (after the 30-day phase correction) and may be used to compute correlations with PVF_2 and $CPVF_2$, with a phase uncertainty of ±5 days.

[11] Figure 3 shows that times of eddy shedding coincide very nearly with maxima in $CPVF_2$ (the maximum lagged correlation coefficient $\gamma \approx 0.6$, shedding lags $CPVF_2$ by about 10 days). The relation can be seen more clearly in Figure 4a, which shows PVF_2 (solid line) and $CPVF_2$ (dotted line) plotted in the same frame, focusing on a shorter, 2000-day period bracketed by the vertical dotted lines in Figure 3. That the Loop Current tends to retract and then sheds an eddy near the end of cumulative influx of cyclonic VFA (i.e., near a maximum of $CPVF_2$) agrees with C2002's and C2003's findings. However, it does not necessarily follow that cyclonic vorticity influx causes the Loop Current to retract or shed an eddy. Another way of highlighting the same information is to plot (Figure 4b) histograms of the number of shed eddies as functions that measure the deviation of PVF_2 (top panel) and $CPVF_2$ (bottom panel) from their respective local maxima: negative (positive) for anticyclonic (cyclonic) influxes (equation (6)). Figure 4b shows that 17 of the total of 18 eddies were shed during anticyclonic PVF_2. On the other hand, the shed eddies cluster about the maxima of the $CPVF_2$ (i.e., about zero-deviation).

[12] In general, a (time) series leads its time-integral. In the case of PVF_2 and its time-integral $CPVF_2$, we find that the former leads the latter by 30∼70 days (see, e.g., Figure 4a). The maximum γ is = 0.65 and occurs at a lag = 50 days ($CPVF_2$ lags PVF_2). Note that this 50-day lag is shorter than one quarter (i.e., $\pi/2$, the lag for a perfect sinusoidal series) of the shedding period (∼270 days). It follows then that shedding occurs some 40∼80 days after

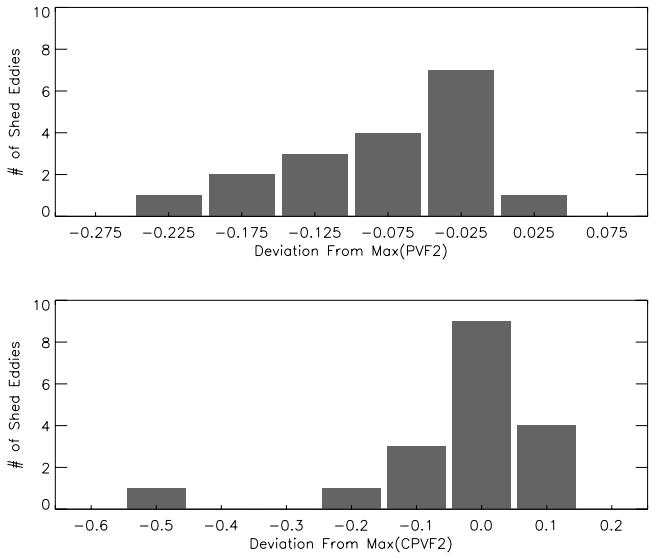

Figure 4b. Histograms of the number of shed eddies as functions of the deviation of (top) PVF_2 and (bottom) $CPVF_2$ from their respective local maxima: negative (positive) for anticyclonic (cyclonic) influxes (see equation (6) and subsequent text).

the beginning of an influx of anticyclonic VFA at the channel, i.e., after a maximum in PVF_2. The maximum lagged correlation γ (at 60 days lag) between PVF_2 and shedding in this case is $\approx$0.55. This same reasoning may be applied to the observed time series. C2002 noted sheddings and retractions near local maxima of $CPVF_2$ (i.e., at ends of cumulative influxes of cyclonic VFA), which suggests that these events occurred sometime during a period of influx of anticyclonic VFA at the Yucatan Channel.

3. CANEK Observations and Satellite SSH

[13] The preceding analyses indicate that cumulative influx lags influx by less than a quarter of the shedding cycle (i.e., by 30$\sim$70 days in the model). The real ocean is much more complex. However, the existence of a lag is almost certain (unless the time series is completely random). A reanalysis of C2002's data is given in Figure 5. This shows 30-day low-passed time series of observed flux of horizontal shear PVF_2 (solid line) and time-integral of this flux $CPVF_2$ (dotted line) during the indicated dates. (The conclusion is unchanged whether 30-day or 50-day low pass (used for the modeled PVF_2) is used. The 30-day low pass is used because it retains details near the end portions of this relatively short observed time series.) The $CPVF_2$ curve is identical to that shown in the lower panel of C2002's Figures 4a–4b, while the PVF_2 curve is the "smoothed"

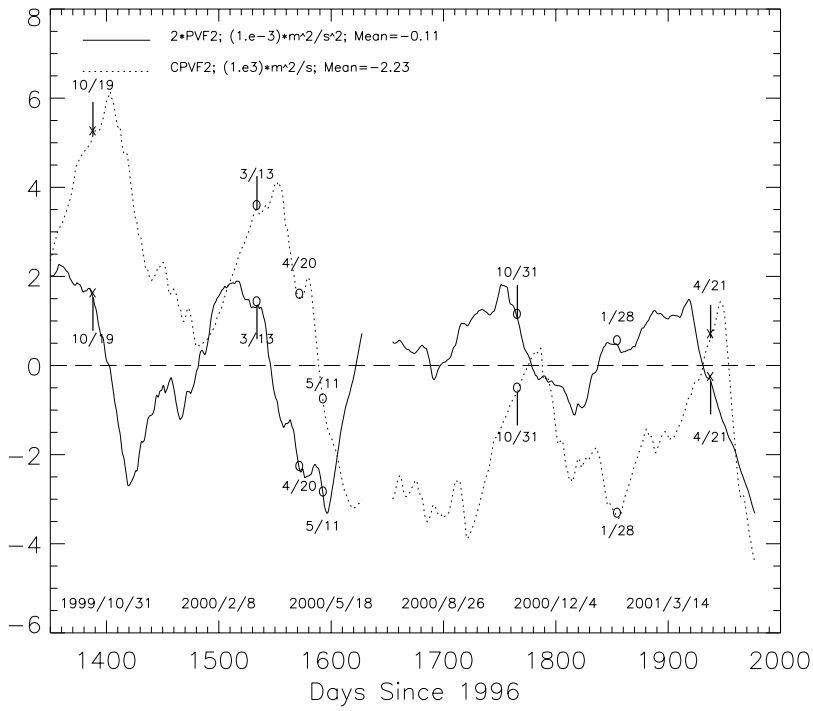

Figure 5. The 30-day low-passed time series of observed flux of horizontal shear $PVF_2 = -\int\int v\frac{\partial v}{\partial x}\frac{\partial r}{\partial z}/r_o dxdz$ (solid line) and time-integral of this flux $CPVF_2 = \int PVF_2 dt$ (dotted line) during the indicated dates. The time-mean of each series is indicated and has been removed. For clarity, the PVF_2 is multiplied by 2. The crosses on each curve indicate actual times the observed Loop Current shed eddies. The circles indicate times when the Loop Current "retracted" but did not actually shed an eddy, as seen from satellite-derived SSH contours. Figure 6 shows an example of this retraction scenario. The short vertical lines correspond to times of either eddy shedding or retraction described by *Candela et al.* [2002]. Month/day of each event is indicated as discussed in text. Data are courtesy of Julio Candela, CICESE.

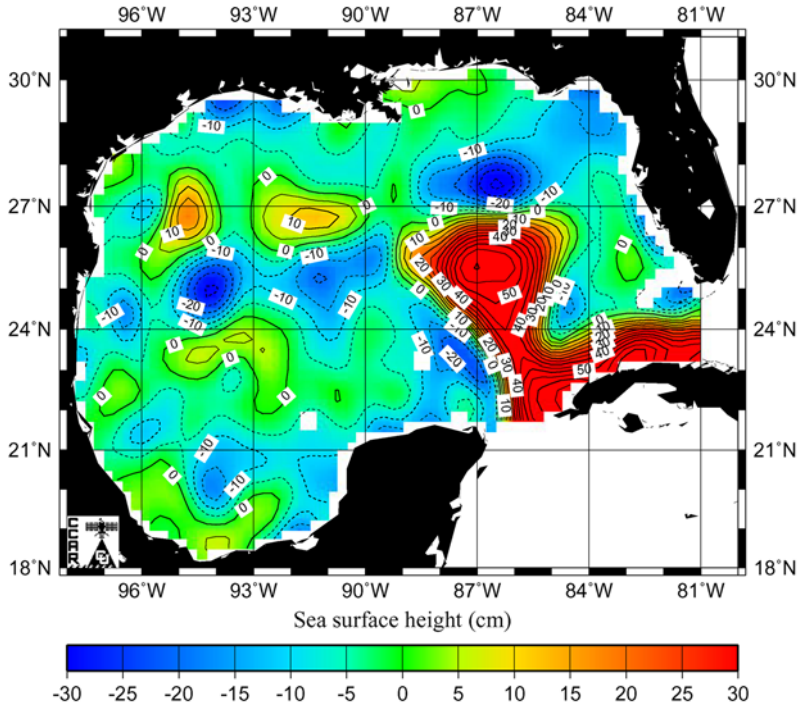

Figure 6. Satellite-derived sea-surface height on 31 October 2000 indicating the Loop Current in a "retraction mode." Image is courtesy of Robert Leben, University of Colorado (http://www-ccar.colorado.edu/~realtime/gsfc_gom-real-time_ssh/).

version of the original PVF_2 time series shown in the upper panel of C2002's Figures 4a–4b. In Figure 5, crosses on each curve indicate the two times when the Loop Current was observed to shed rings, on (approximately) 19 October 1999 and 21 April 2001. The short vertical lines correspond to the four times described in C2002 when the Loop Current either shed eddies (i.e., 19 October 1999 and 21 April 2001) or when it retracted and developed a "neck" near its base

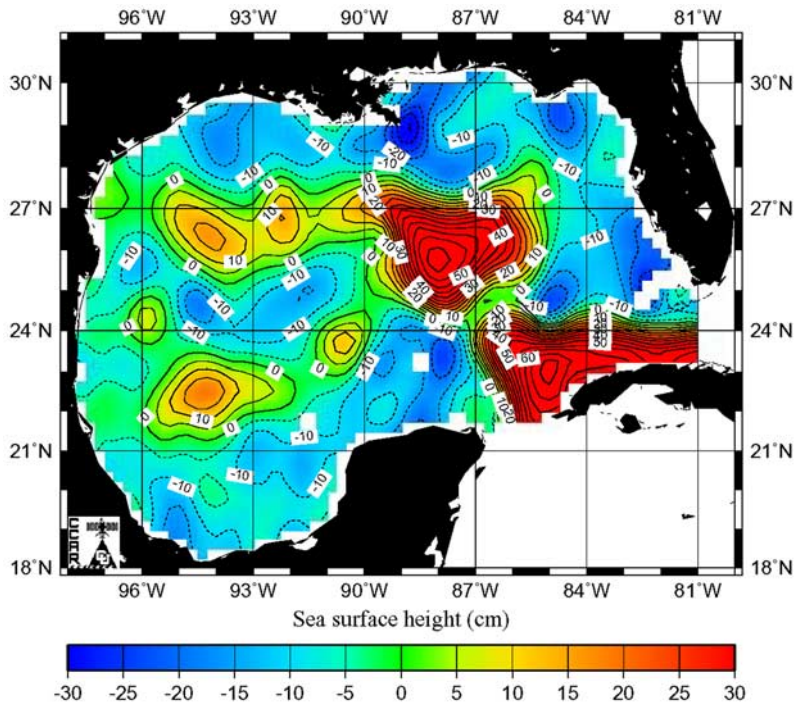

Figure 7. Satellite-derived sea-surface height on 28 January 2001 indicating the Loop Current in a retraction mode, and a ring that is temporarily detached from the Loop Current.

immediately north of the Yucatan Channel (13 March 2000 and 31 October 2000). The behaviors of the Loop Current (i.e., whether it sheds rings or retracts, or otherwise extends) are inferred from satellite-derived SSH maps from Robert Leben's website (http://www-ccar.colorado.edu/~realtime/gsfc_gom-real-time_ssh/). An example for the 31 October 2000 retraction case is shown in Figure 6. As noted by C2002, and indicated in Figure 5 by the four short vertical lines, shedding and/or retraction occurred near times of local highs in the $CPVF_2$ curve. Figure 5 also shows that the observed $CPVF_2$ lags PVF_2 by 30~50 days. This (lagging) result is consistent with the model analysis discussed in the previous section. Figure 5 indicates that the four observed retraction and eddy shedding events actually occurred some 10~30 days after influxes of anticyclonic (i.e., coincident with downward trends in the PVF_2 curve), rather than cyclonic VFA.

[14] The relation between Loop Current shedding/retraction events with PVF_2 (or $CPVF_2$, i.e., Figure 5) is now examined in more details in conjunction with daily maps of satellite-derived SSH during the period of C2002's observations. I find at least three additional instances (other than those considered in C2002) when retractions of the Loop Current did not occur near times of local highs in the $CPVF_2$ curve. These times are marked by circles without the vertical short lines in Figure 5: 20 April 2000, 11 May 2000 and 28 January 2001. The last of this, in fact, corresponded to a time when the retraction was sufficiently severe that a ring temporarily detached (for about 10 days) from the Loop Current (Figure 7). Contrary to the four previous cases, all three new cases occurred long (>30 days) past the local maxima of $CPVF_2$, near times of either local lows or downward trend in the $CPVF_2$ curve, i.e., during times of influx and accumulation of anticyclonic vorticity. The first two cases (20 April and 11 May 2000) occurred when there were also influxes of anticyclonic VFA (i.e., coincident with downward trend in the PVF_2 curve), consistent with the previous four cases. The 28 January 2001 case actually occurred during a period of generally upward trend in PVF_2, though locally the curve shows a plateau indicative of a short burst of anticyclonic VFA influx. These observations, with perhaps the exception of the 28 January 2001 case, indicate then that Loop Current eddy shedding or retraction tends to occur at instances when there is an influx of anticyclonic VFA. Shedding or retraction tends to occur shortly (10~30 days) after a local maximum of PVF_2, suggestive (but not proof) that an increased influx of anticyclonic VFA perhaps initiates Loop Current eddy shedding or retraction. In five of the seven cases (exceptions are 20 April and 11 May 2000), shedding or retraction is preceded by a more prolonged period of influx of cyclonic vorticity (Figure 5). These inferences generally agree with those derived previously from the model analyses (e.g., Figure 3 or 4a–4b), though there are some significant differences. The model sheds eddies more or less regularly (every 9 months). Although the corresponding VFA time series (Figure 3) contain shorter-period fluctuations that represent model Loop Current retractions (and extensions), they are generally of smaller amplitudes (than VFA fluctuations caused by main shedding events). In other words, these smaller events do not significantly affect the correlations between model shedding and VFA. On the other hand, there were only two sheddings during the CANEK observation, separated by about 17 months, and Loop Current retraction events are of similar amplitudes (as sheddings; Figure 5). These differences between modeled and observed Loop Current behaviors not only contribute to differences in the relative phasing between shedding (retraction) and VFA, but also are reminders that the real ocean is truly very complex.

4. Conclusion

[15] On the basis of analyses of a 15-year model simulation with simple forcing, CANEK observations across the Yucatan Channel, and satellite-derived SSH maps in the Gulf of Mexico, this study attempts to relate VFA at the Yucatan Channel with Loop Current variability and eddy shedding. Observations indicate that Loop Current retraction and eddy shedding normally occurred near the end of an extended period of cyclonic influx of $CPVF_2$, but this is not always the case, and at least three of the seven events that were identified show retractions occurring at times of anticyclonic influx of $CPVF_2$. On the other hand, PVF_2 might be a more suitable indicator as six of the seven events occurred at times of anticyclonic influx of PVF_2, and one event occurred during a short burst of anticyclonic PVF_2 influx. These inferences are in general agreements with the model analyses. The scenario that cyclonic influx of VFA extends the Loop Current (thus making the Loop Current more susceptible to retract or shed an eddy) and influx of anticyclonic VFA "triggers" retraction or even eddy shedding seems to be also consistent with Reid's simple model based on PV-conservation. However, the converse may not be true; that is, the simple model has not explained why the Loop Current retracts or sheds eddies.

[16] While the present analysis provides some insights into the relation between VFA and Loop Current variability, it seems doubtful that complex Loop Current behaviors can be wholly explained in terms of flow conditions at Yucatan (O2003 expressed similar doubts). To more thoroughly understand and quantify the phenomenon, one would need much longer observational data, coupled with high-resolution modeling specified with more realistic forcings.

[17] The issue of good resolution especially in the core current is important. As mentioned previously, the calculation of PVF_2 (and $CPVF_2$) is dominated by flow values near the surface at the western portion of the channel. Inadequate resolution (in observations and/or models) can result in large uncertainty when estimating horizontal shears. This may be the case with the 2~3 current-meter moorings in the observational data set [*Candela et al.*, 2002]. The present model, with about 5~6 grid points across the region of strong shears, only fairs slightly better.

[18] **Acknowledgments.** Comments from the three reviewers were very useful. I also benefited from discussions with Jose Ochoa, Julio Candela, and Julio Sheinbaum. Jose Ochoa suggested alternative interpretations of the vq_2 flux integral, and Julio Candela graciously provided me with the CANEK data and his unpublished plots. I also appreciate comments from Chris Mooers and Tal Ezer. This work was supported by the Office of Naval Research and the Minerals Management Service. Computing was done at GFDL/NOAA, Princeton.

References

Candela, J., J. Sheinbaum, J. L. Ochoa, A. Badan, and R. Leben (2002), The potential vorticity flux through the Yucatan Channel and the Loop Current in the Gulf of Mexico, *Geophys. Res. Lett.*, *29*(22), 2059, doi:10.1029/2002GL015587.

Candela, J., S. Tanahara, M. Crepon, B. Barnier, and J. Sheinbaum (2003), Yucatan Channel flow: Observations versus CLIPPER ATL6 and MERCATOR PAM models, *J. Geophys. Res.*, *108*(C12), 3385, doi:10.1029/2003JC001961.

Elliott, B. A. (1982), Anticyclonic rings in the Gulf of Mexico, *J. Phys. Oceanogr.*, *12*, 1292–1309.

Hurlburt, H. E., and J. D. Thompson (1980), A numerical study of Loop Current intrusions and eddy shedding, *J. Phys. Oceanogr.*, *10*, 1611–1651.

Oey, L.-Y., H.-C. Lee, and W. J. Schmitz Jr. (2003), Effects of winds and Caribbean eddies on the frequency of Loop Current eddy shedding: A numerical model study, *J. Geophys. Res.*, *108*(C10), 3324, doi:10.1029/2002JC001698.

Reid, R. O. (1972), A simple dynamic model of the Loop Current, in *Contributions on the Physical Oceanography of the Gulf of Mexico*, vol. II, edited by L. R. A. Capurro and J. L. Reid, pp. 157–159, Gulf, Houston, Tex.

Schmitz, W. J., Jr. (1996), On the world ocean circulation, vol. I, Some global features/North Atlantic circulation, *Tech. Rep. WHOI-96*-03, 141 pp., Woods Hole Oceanogr. Inst., Woods Hole, Mass.

Sturges, W., and R. Leben (2000), Frequency of ring separations from the Loop Current in the Gulf of Mexico: A revised estimate, *J. Phys. Oceanogr.*, *30*, 1814–1818.

Teague, W. J., M. J. Carron, and P. J. Hogan (1990), A comparison between the Generalized Digital Environmental Model and Levitus climatologies, *J. Geophys. Res.*, *95*, 7167–7183.

L.-Y. Oey, Princeton University, P.O. Box CN 710, Sayre Hall, Princeton, NJ 08544, USA. (lyo@princeton.edu)